AD-A056 954 INDIANA UNIV AT BLOOMINGTON DEPT OF CHEMISTRY F/G 7/4
INVESTIGATION INTO THE OPERATING CHARACTERISTICS OF A MICROARC --ETC(U)
JUL 78 R I BYSTROFF, L R LAYMAN, G M HIEFTJE N00014-76-C-0838
UNCLASSIFIED TR-14 NL

| OF |
AD
A056954

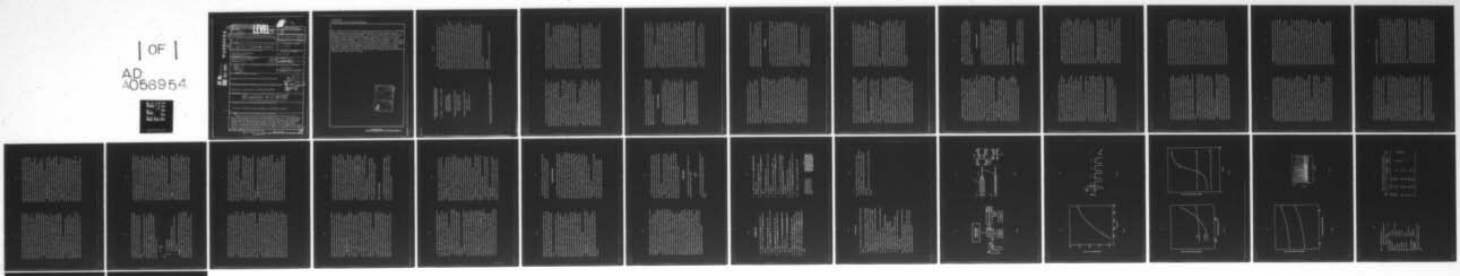

END
DATE
FILMED
9 -78
DDC

AD A056954

AD No. ____
DDC FILE COPY

SECURITY CLASSIFICATION OF THIS PAGE (When Data Entered)

(14) TR-14 REPORT DOCUMENTATION PAGE

LEVEL II

READ INSTRUCTIONS BEFORE COMPLETING FORM

1. REPORT NUMBER: Fourteen
2. GOVT ACCESSION NO.
3. RECIPIENT'S CATALOG NUMBER (9)

4. TITLE (and Subtitle) (6)
Investigation into the Operating Characteristics of a Microarc Atmospheric-Pressure Glow Discharge.

5. TYPE OF REPORT & PERIOD COVERED
Interim Technical Report, (13)

6. PERFORMING ORG. REPORT NUMBER
19

7. AUTHOR(s) (10)
R. I. Bystroff, L. R. Layman and G. M. Hieftje

8. CONTRACT OR GRANT NUMBER(s)
N14-76-C0838

9. PERFORMING ORGANIZATION NAME AND ADDRESS
Department of Chmiestry
Indiana University
Bloomington, In 47401

10. PROGRAM ELEMENT, PROJECT, TASK AREA & WORK UNIT NUMBERS
NR 051-622

11. CONTROLLING OFFICE NAME AND ADDRESS
Office of Naval Research
Washington, D.C.

(11) 24

12. REPORT DATE
July 24, 1978

13. NUMBER OF PAGES
46

14. MONITORING AGENCY NAME & ADDRESS (if different from Controlling Office)
(12) 26p.

15. SECURITY CLASS. (of this report)
Unclassified

15a. DECLASSIFICATION/DOWNGRADING SCHEDULE

16. DISTRIBUTION STATEMENT (of this Report)
Approved for public release; distribution unlimited

DDC RECEIVED AUG 2 1978 F

17. DISTRIBUTION STATEMENT (of the abstract entered in Block 20, if different from Report)
Prepared for publication in APPLIED SPECTROSCOPY

18. SUPPLEMENTARY NOTES
(15) N00014-76-C-0838

19. KEY WORDS (Continue on reverse side if necessary and identify by block number)
Microarc, atomization, glow discharge, multielement analysis

20. ABSTRACT (Continue on reverse side if necessary and identify by block number)
Details of the processes occurring during sample atomization from a 'microarc' discharge have been studied photometrically, by use of high-speed color cinematography and through current-voltage waveforms. The 'microarc' studied here is an atmospheric pressure inert gas glow discharge supported between 0.25 mm diameter tungsten wires; quiescent argon-1% H_2 provides reactive-sputtering conditions and improved behavior in the presence of oxygen impurities. Excitation temperatures of ca. 5000°K are measured for the argon

DD FORM 1 JAN 73 1473 EDITION OF 1 NOV 65 IS OBSOLETE
S/N 0102-014-6601

UNCLASSIFIED
SECURITY CLASSIFICATION OF THIS PAGE (When Data Entered)

176 685

glow. Samples of Na, Al and Sr illustrate the influence of volatile, refractory, insulating and electron-emitting sample properties on the temporal-spatial-electrical behavior of the discharge. The step-by-step events occurring in the discharge are described qualitatively and a variety of processes are invoked to explain sample volatilization, including sputtering, chemical reactions and purely thermal effects. In the first stages of the discharge, stabilities are related to the placement and insulating character of deposits. With heating electron emission becomes important in directing the discharge to or away from the sample; abnormal glow wandering and glow-to-arc transitions can ensue. Improved stability is achieved by uniformly depositing multielement samples along the electrode, which localizes the initial discharge and promotes ablative cooling of the sample and electrode.

INVESTIGATION INTO THE OPERATING CHARACTERISTICS OF A "MICROARC" ATMOSPHERIC-PRESSURE GLOW DISCHARGE*

R. I. Bystroff, L. R. Layman†, and G. M. Hieftje††

Department of Chemistry
Lawrence Livermore Laboratory
Livermore, California 94550

†Permanent address: Department of Chemistry,
Pacific Lutheran University
Tacoma, Washington 98447

††Permanent adress: Department of Chemistry,
Indiana University
Bloomington, Indiana 47401

*Work performed under the auspices of the U.S. Department of Energy by the Lawrence Livermore Laboratory under contract number W-7405-ENG-48.

Abstract

Details of the processes occurring during sample atomization from a "microarc" discharge have been studied photometrically, by use of high-speed color cinematography and through current-voltage waveforms. The "microarc" studied here is an atmospheric pressure inert gas glow discharge supported between 0.25 mm diameter tungsten wires; quiescent argon-1% H_2 provides reactive-sputtering conditions and improved behavior in the prescence of oxygen impurities. Excitation temperatures of ca. 5000°K are measured for the argon glow. Samples of Na, Al and Sr illustrate the influence of volatile, refractory, insulating and electron-emitting sample properties on the temporal-spatial-electrical behavior of the discharge. The step-by-step events occurring in the discharge are described qualitatively and a variety of processes are invoked to explain sample volatilization, including sputtering, chemical reactions and purely thermal effects. In the first stages of the discharge, instabilities are related to the placement and insulating character of deposits. With heating, electron emission becomes important in directing the discharge to or away from the sample; abnormal glow wandering and glow-to-arc transitions can ensue. Improved stability is achieved by uniformly depositing multielement samples along the electrode, which localizes the initial discharge and promotes ablative cooling of the sample and electrode.

Index Headings:

Microarc, atomization, glow discharge, multielement analysis.

One of the most active current endeavors in analytical chemistry is the search for new methods of multi-element analysis. Improvements in many existing methods have been proposed and new ones developed. Perhaps the most significant of these advances has been the recent emergence of the inductively coupled plasma as a tool for multi-element determinations (1). However, this new, powerful source has been found to have limitations and the search for alternative techniques continues.

Ideally, whatever approach is finally adopted in a multi-element scheme should be amenable to use with any detection technique. That is, it should be possible to employ for atom detection an atomic fluorescence method, atomic emission, or even ion detection (2). The key to such flexibility is to develop a device for generating atoms which is useful under a variety of conditions and with any of the detection methods. One promising such atomizer is the so-called microarc (3).

The microarc, as originally configured, is essentially an atmospheric-pressure glow discharge operating in an argon environment. The discharge is characterized by relatively high voltages, controlled currents, and a sputtering kind of atom formation process. Coupled with a microwave plasma excitation source, the microarc has been shown to yield high sensitivity, low susceptibility to matrix interferences, reproducibility of atom formation, low sample volume requirements, and the capability of operation at atmospheric pressure. However, this new discharge offers other potential advantages as well. The microarc could serve as an excitation

source as well as sample atomizer to possible provide many of the advantages it previously exhibited but in a simpler configuration. Finally, the device is readily controlled and should be easily automated.

To realize the potential of this new kind of discharge, it must be studied and understood more completely. In the present investigation, a discharge similar to the microarc was constructed and placed under careful control. A reproducible electrode arrangement, employing tungsten wires, was configured in a chamber which enabled a controlled atmosphere (primarily argon) to be utilized at atmospheric and slightly lower pressures. With this new system, the character and stability of the resulting discharge, electrode erosion behavior, sample volatilization and sample atomization were all studied as functions of discharge voltage, current, waveform, electrode surface condition and chemical state, environmental gas composition, and the size, chemical composition, and physical nature of the sample.

In the studies, it was found that electrode temperature and surface character play an important part in the formation and stabilization of the microarc kind of sputtering discharge. To maintain the discharge and minimize electrode erosion, it is essential that oxidation of the electrode wire be minimized. In turn, tungsten oxidation can be minimized in this discharge by addition of small amounts of hydrogen gas to the argon atmosphere. For optimal discharge stability, reproducibility, and simplicity of operation, discharge-initiating electrons should be provided,

the sample coated thinly and uniformly over the electrode, and the discharge current controlled carefully. The consequences of these findings and their importance to the practical utilization of the microarc in a multi-element scheme will be considered and discussed in detail.

NATURE OF THE MICROARC

Because the microarc is a new kind of analytical discharge, it is instructive to review its basic characteristics and to compare it with the conventional glow discharge, to which it is most similar. In many respects, the microarc is merely an atmospheric-pressure glow discharge, but its relatively high pressure alters the current-voltage characteristics and spatial dimensions of the glow. Moreover, the unusual electrode materials and configuration employed in the microarc and the temporal variations exhibited by the new discharge make it quite unique. In this section, the similarities and differences between the microarc and glow discharge will be reviewed.

Many of the characteristics of low-pressure glow discharges can be extrapolated to the regime in which the microarc operates. These conventional discharges have been extensively studied and described (4-7) and the special characteristics of the hollow cathode glow were recently considered in the excellent review of Slevin and Harrison (8). In these

studies, a set of "similarity laws" have been found to describe the relation of discharge pressure (P) to the electric field (E), the length of the cathode fall (d) and the discharge current density (j). Specifically, over a broad range in pressure, E/P, $P \cdot d$ and j/P^2 tend to remain constant in a glow sustained by secondary emission.

The proportionality between electric field and pressure implies that the energy acquired by ions and electrons over one mean free path is independent of pressure. In addition, the inverse dependence of cathode fall (d) on pressure signifies that the same number (ca. 100) of mean free paths exists in either pressure regime. Consequently, the length of the cathode fall in the microarc will be small but in keeping with the overall reduced dimensions of the high-pressure configuration. Also, the contraction of d at increasing pressures implies the existence of very high fields in the neighborhood of the cathode surface, with the inevitable result that field emission becomes an important source of electrons from the surface at fields approaching 10^6 volts/centimeter (9). Consequently, high-pressure glows are sensitive to microscopic cathode surface roughness and to small differences in work function of the cathode material and tend to relax into arc-type discharges. Such phenomena, which have been observed in tungsten-supported air glows (10), require that the microarc be closely controlled and that the cathode material might strongly affect the discharge features.

Because the current density (j) increases as the square of the discharge pressure, the atmospheric-pressure microarc can carry relatively large currents even though its electrode surface area is quite small.

Obviously, this increased current density increases the rate of volatilization of electrode material and, more importantly, any sample material placed on it. Moreover, relatively high surface and gas temperatures are generated in the region of the cathode fall, suggesting that current density will more probably change in proportion to $P^{4/3}$ as shown by von Engle (11).

In addition to differences expected because of its atmospheric-pressure operation, the microarc possesses many features which should make it unlike the classical glow. Most importantly, the microarc cathode is not planar, as assumed in most treatments of the glow, but consists of a conductive, bent metal wire, which has been partially coated with dielectric sample material. The discharge character would thus be expected to be strongly affected by sample material, the thickness of the coating, and the distribution of sample over the electrode. In addition, volatilization of the sample would be expected to change the discharge with time. Clearly, volatilized sample material might either hinder or enhance the discharge and might even dominate the current carrying-species in the discharge. Finally, thermionic emission from the cathode should strongly affect the microarc and would be expected to change as the electrode heats during the discharge.

Obviously, the differences between the microarc and coventional glow discharges preclude any simple extrapolation of previously observed behavior. Accordingly, the present study has been separated into two segments dealing respectively with characterizing the microarc alone and in observing the discharge after the introduction of sample material. These initial studies are intended to be exploratory and necessarily descriptive

and merely indicate directions for more intensive research into the basic processes occurring in the microarc. For this reason, a controlled-environment discharge chamber was constructed and a number of qualitative, quantitative and semi-quantitative observations made. This apparatus and the measurement techniques are described in the next section.

EXPERIMENTAL

A block design of some of the instrumentation employed in the microarc investigation is shown in Figure 1. The microarc chamber, to be described in more detail below, housed the microarc electrodes and provided a controlled-atmosphere environment in which the discharge could be studied. Hydrogen (commercial grade) and Argon (prepurified) gases necessary for microarc operation were controlled by double-stage regulators, metered by suitable needle valves, and allowed to mix by diffusion in the chamber. A mechanical vacuum pump (Duo-Seal, M. W. Welch Co., Chicago, IL), equipped with a liquid nitrogen trap and vacuum control (type 77, MKS Instruments Co., Burlington, Mass) were used to establish the desired static chamber pressure. A programmable microarc power supply, also discussed below, provided voltages and currents of the desired amplitude and waveform for driving the microarc.

For spectrometric monitoring of microarc emission, a small monochromator (model EU-700, McPherson Instrument Co., Acton, MA) and photomultiplier (R456, Hamamatsu TV, Ltd.) were employed. The monochromator's entrance and exit slits were held at 10 μm (~0.2 A

spectral bandwidth) in all measurements and the photomultiplier was supplied with -800 V by a suitable power unit (model EU-42A, McPherson Instrument Co., Acton, MA). A picoammeter (model 414A, Kiethley Instruments, Cleveland, OH) served to indicate output photocurrents. To enable the measurement of absolute spectral radiances from the microarc, the entire photometric system was calibrated with an NBS-certified tungsten ribbon lamp operated at 2850°C.

Microarc Chamber and Electrode Assembly. The microarc chamber was constructed of anodized aluminum and in design consisted of a hollow 4 in. cube, having six face-centered circular holes each with a 3 in. clear aperture. In these holes, gas inlets, vacuum and electrical connections, and viewing ports (quartz) were mounted.

Electrode mounting assemblies for the microarc were designed to enable accurate, reproducible placement of the electrodes at specified distances from each other and at prescribed locations on the photometric viewing axis. These assemblies, shown in Figure 2, are comprised of the electrodes themselves (anode and cathode) and a syringe-based positioning arrangement. Each electrode was constructed of a hairpin-shaped loop of 0.25 mm tungsten wire (total length of each = 30 cm), having 99.95% purity. At its sharpest bend, the radius of curvature of each electrode was approximately 1 mm. The end of the cathode was enclosed in 3 mm Pyrex via a graded seal, to permit its stable positioning in a feedthrough. However, the anode was sealed (graded) into the Pyrex plunger of a 2 mL laboratory syringe; rigidly fastening the syringe barrel to the electrode chamber via another feedthrough then enabled the anode to be positioned anywhere along a

straight line parallel to he barrel axis. Spacers between the barrel and plunger terminus provided reproducible selection of this position. In addition, rotation of the anode could be employed to exactly establish desired interelectrode distances; a cathetometer with x,y positioning readable to ±4 μm aided in measuring this gap and in observing the negative glow. Electrode wires within each respective glass enclosure were insulated from each other by means of glass capillary sleeves.

To ensure reproducible discharge initiation, the anode wire was heated resistively using an ac current applied from an autotransformer. Although different anode temperatures were explored, 985°C was chosen as the best value on the basis of discharge consistancy and was employed in most investigations.

Microarc Power Supply. The discharge was driven by a specially constructed power supply capable of DC, full-wave, full-wave rectified or half-wave rectified modes of operation. The maximum voltage was 1200 VAC or 800 VDC and a variety of ballast resistors provided constant current control up to a maximum of 200 mA. An additional feature of the supply was its control of the discharge on a cycle-by-cycle basis, accomplished with zero cross-over sense switches, and high voltage vacuum relays. Control programs were written in BASIC and executed by an Intel 8080 micropropessor integrated into the controlled power supply. Such duty factor control was useful in pyrometric studies of temperature and in observing the early part of the discharge.

Additional Discharge Monitoring. Two methods other than photometric monitoring (cf. Figure 1) were employed to characterize the microarc discharge. For high-resolution spatial mapping of the time-averaged discharge behavior a 128-element linear photodiode array (Reticon Corp., Sunnyvale, CA) was used, whereas general discharge features were time-resolved with the aid of high-speed cinematography. An image of a portion of the discharge was formed on the photodiode array through a single interference filter (10.0 nm bandpass, tricavity, IR blocked, Pomfret Research Corp., Stamford, Conn.) with the aid of a dual convex lens system.

High speed motion pictures were obtained with a framing camera (model DBMSB, D. B. Millikan Co., Arcadia, CA) having nominal framing rates of 400 and 200 Hz. Timing marks on the film aided in the interpretation. A 50 mm Switar f/1.8 lens was employed. The ASA 125 film was Kodak Ektrachrome Type 7240 and EF, color balanced for tungsten at 3200°K, which use VNF-1 and E-2 processing, respectively.

Procedure. All investigations were performed with the microarc operating in a quiescent environment. To prepare the electrodes for each study, the following procedure was employed: (1) A "pre-burn" in argon-1% H_2 at reduced pressure (~0.5 atm) for several minutes was employed to assure surface cleanliness, (2) The sample was loaded while a slight positive pressure of argon was maintained in the chamber, (3) The sample electrode was resistively heated to evaporate the water, (4) The chamber was evacuated until outgassing of the water was negligible (<5 microns/min), (5) Hydrogen and argon were added to the desired pressures.

Reagents. Reagent grade sodium chloride, strontium nitrate and aluminum nitrate were used in preparing stock solutions in deionized water at the 10 ppm to 100 ppm concentration levels. A graduated 10 µL Hamilton hypodermic syringe was employed in transferring known quantities to the sample electrode.

RESULTS AND DISCUSSION

As indicated above, the unusual geometry and degree of complexity of the microarc demand that the discharge be studied by itself before the effect of sample material on its characteristics is determined. Accordingly, the discharge was first investigated in a pure argon environment at pressures slightly below atmospheric. This slightly reduced pressure (0.8 atm) expanded the discharge slightly and enabled its simpler characterization while leaving its basic features unchanged. In addition, the static atmosphere provided by the enclosure (described earlier) enabled discharge stability to be increased and permitted time-dependent behavior to be more readily observed. Later, solids were added to the cathode in the form of dissolved solutes to enable the effect of sample material on the discharge to be ascertained.

The Microarc Without Sample Material

Appearance of the Discharge. By itself, the 0.8 atm microarc has all the features of a conventional glow discharge, including a dark cathode fall region ending in a blue negative glow and, progressing toward the anode, the

Faraday dark space and a narrow (constricted) positive column (or arc column). In the pulsating discharge, the negative glow region in pure argon was sharply defined during the first 0.5 seconds, after which it became progressively more diffuse as the cathode wire slowly heated to incandescence. The distance between the cathode and the negative glow region (i.e., the cathode fall distance, d) was quite small at this elevated pressure and was estimated by extrapolation from measurements of its dimensions made at lower pressures. The inverse relationship between the cathode fall distance and pressure renders this extrapolation quite straightforward; the resulting value, along with a number of other discharge parameters discussed below, is shown in Table 1.

At small interelectrode distances the positive column disappeared, and the cathode fall could be measured as 180 V (cf. Table 1), a value consistent with both measured and calculated cathode falls for argon planar glow discharges at low pressures (12). However, as interelectrode distances increased, the discharge voltage was observed to increase because of the resistive drop in the arc column. Moreover, this positive column is noted to fragment into an odd number of arcs when discharge current was increased; not unexpectedly, the arcs centered at the narrowest point between the electrodes.

The current density, listed in Table 1 was estimated from the maximum area of the glow and the peak current achieved within a discharge cycle. This value is consistent with those previously reported (5, p. 202) if a $P^{4/3}$ scaling relationship is employed, as suggested earlier.

Discharge Temperature. Because the microarc is expected to find application principally in the atomization of samples, translational or kinetic temperatures would be expected to be most useful in characterizing its behavior. However, because the microarc operates at or near atomspheric pressure, such temperatures would be assumed to lie close to excitation temperatures, which are far more redily measured. Accordingly, the multiple-line (slope) technique for excitation temperature measurement was employed in this study (13). To perform these measurements, the discharge was imaged with unity magnifiction onto the entrance slit of the monochromator in the calibrated photometric system depicted in Figure 1. Corrected emission intensities of several argon spectral lines were then determined and correlated with tabulated transition probabilities (14). The slope of the resulting plot indicated that the temperature within the negative glow (with 10 μm spatial resolution) was 5000 ± 200°K (cf. Table 1).

Cathode Wire Temperature. An optical pyrometer with 0.25 mm spatial resolution was employed to determine the temperatures along the cathode wire. Obviously, the temperature and its profile changes with the duration of the discharge, to produce the behavior shown in Figure 3. Figure 3 reveals the typical behavior of the maximum wire temperature with time for a pulsating half wave or full wave rectified discharge.

Temperature gradients along the microarc cathode wire can be as high as 200°K/mm. However, such gradients are strong functions of the gap dimensions and current of the discharge. Small electrode gaps encourage localized heating and large gradients, since the arc channel plays a primary

role in cathode heating. In contrast, the more uniform glow produced at large interelectrode distances (1 mm) generates less pronounced temperature gradients. As in most glows, the discharge power is almost entirely delivered to the cathode and little or no erosion of the anode occurs. Because the anode is independently provided with resistive heating, its temperature does not change noticably. From a practical standpoint these findings imply that cathode erosion in the microarc can be minimized by maintaining an interelectrode distance large enough or a discharge current low enough to minimize the formation of concentrated arc channels. Regardless of interelectrode spacing, however, anode lifetime should pose no problem.

Microarc Breakdown Voltage. The striking or breakdown voltage of the microarc is of interest solely because it determines the minimum voltage of the power supply used to drive the discharge. We have found this voltage to be linearly dependent on the electrode gap, although it can be reduced substantially when ions or electrons are present. In the present study, such electrons were generated by thermionic emission from the resistively heated anode, and assured a manageable (1 kV) breakdown potential for interelectrode gaps less than 1 mm.

Current-Voltage Characteristics of the Microarc. A distinction between microarc behavior and that of the conventional glow discharge can be most readily seen from examining the current-voltage characteristics of the two. Whereas a glow would be expected to exhibit a constant voltage as discharge current is increased, the microarc voltage exhibits a slight dependence on discharge current, betraying its slightly arc-like character. As the

pulsating microarc discharge proceeds, the cathode heats, changing the initial glow-like behavior to something resembling a combination glow/arc plasma. This behavior can be seen in Figure 4, where the early flat-topped voltage waveforms slowly assume a rounded shape as the cathode warms. This behavior can be ascribed to the increasing influence of cathode thermionic emission on the discharge as follows: When a discharge first strikes, the glow can be observed to reside longest at the initial point of discharge. Consequently, more energy is deposited at that point than at any other, heating the cathode locally, encouraging thermionic emission, and anchoring the discharge even more firmly to that spot. Consequently, a large thermal gradient is established along the cathode wire and the discharge current quickly assumes a thermionic component. In turn, the thermionic character promotes a higher current density and lower cathode fall which are characteristic of a transition between a glow and arc plasma. Fortunately, conduction of heat away from the gap prevents relaxation of the discharge into a complete arc, although localized regions of the discharge possess arc character. These time and spatially resolved optical observations are reflected in an integrated fashion in the voltage behavior shown in Figure 4, which contains contributions from all parts of the discharge. Similar features have been observed in the hot hollow cathode discharge (15). The interpretation is consistent with the fact that the rounded wave form observed in the later cycles of Figure 4 can be obtained earlier in the discharge merely by reducing the interelectrode distance to place the arc column nearer the cathode or by strongly heating either electrode to provide an increased thermionic component to the arc current.

Emission Behavior of the Microarc. Because of the mixed arc/glow character of the microarc, it is of interest to determine whether cathode erosion occurs predominately through a sputtering mechanism as in the glow or through thermal volatilization as in the arc. In an effort to answer this question, the effect of discharge current on the intensities of both argon and tungsten lines was established. The slit of the calibrated spectrometer (cf. Fig. 1) was carefully aligned with a section of the negative glow tangent with the cathode wire; corrected intensities of the argon 415.8 nm and tungsten 400.9 nm lines were than compared as the discharge current was increased from 60 to 180 mA. As shown in Figure 5, the ratio of the line intensities remained essentially constant, suggesting a sputtering mechanism. However, at any selected discharge current, anode heating could be employed to increase the degree of arc character in the discharge. As revealed in Figure 6, increasing the anode temperature increased the ratio of tungsten to argon line emission, indicating an increase in thermionic contribution to the discharge and a resultant thermal volatilization of the cathode material.

From a practical standpoint, it would be convenient to be able to vary the contribution of arc- and glow-type discharges to the microarc. Although sputtering is known to be highly effective in volatilizing a wide range of solids, it is a relatively slow process. In contrast, thermal volatilization produced by an arc is somewhat selective and poorly understood, but kinetically superior to sputtering. Unfortunately, as will be shown later, sample material has a strong effect on the arc/glow nature of the microarc, rendering discharge current control even more important.

Influence of Impurities. In the first applications of the microarc (3), little attention was paid to the purity of the tungsten electrodes or to the importance of excluding traces of oxygen from the atmosphere around the discharge. In the present study, high-purity tungsten wire was employed and the influence of oxygen in the discharge was ascertained. In our earliest observations, the formation of microscopic tree-like protuberances on the cathode and the production of blue tungsten oxide deposits in the discharge chamber strongly suggested a contribution from oxygen to volatilization of cathode material. To more carefully characterize the role of oxygen in this process, two experiments were performed. In the first, high-speed motion pictures were taken of the discharge as 0.1 mL of oxygen (equivalent to 80 ppm in the discharge atmosphere when fully diluted) was injected into the dischage chamber. The progess of oxygen diffusing along the electrode wires was then tracked and the glow was seen to change into an unstable arc-like plasma. In the second experiment, the discharge chamber was intentionally allowed to leak, so that atmospheric oxygen slowly diffused to the electrode. At the same time, photometric observations of the negative glow region were made with the system shown in Figure 1. Figure 7 reveals that the infusion of oxygen into the discharge chamber rapidly increased the production of tungsten vapor; independent measurements indicated that this vapor increase began approximately when the cathode reached the temperature range where tungsten oxides vaporize (1300-1500^{o}C). Significantly, the spectrum of the glow during this period of high tungsten volatilization contained no evidence of argon or tungsten oxide emission (16), but only that of tungsten atoms. These observations suggest both that

the rapidly volatilizing tungsten (or its oxide) assumed the role of principal current carrier in the discharge and, furthermore, that tungsten oxide which was volatilized from the cathode was rapidly and perhaps quantatively decomposed to the metal during or immediately after its volatilization. Similar observations of the chemical role of trace oxygen have been made by others (17).

Because such erosion of the microarc cathode is highly undesirable, 1% hydrogen gas was added to the argon in the discharge chamber, in an effort to "getter" the oxygen before it could react with the tungsten electrode. With hydrogen present, tungsten emission was greatly reduced and showed little change with cathode temperature (cf. Figure 7) confirming the efficiency of hydrogen as an effective oxygen getter and that the water and OH which are produced during the reaction do not affect electrode surface materially. Because of the sensitivity of the electrode to oxygen, 1% hydrogen was added to the discharge gas, and prepurified argon (<20 ppm O_2) was employed in all subsequent studies. Significantly, the addition of hydrogen to the discharge atmosphere is effective in cleaning the wire surface. Although embrittlement of the wire after extensive use was noted, hydrogen is not expected to be responsible (18); embrittlement is attributable to tungsten metal phase changes which occur during temperature cycling.

To determine the effect of vacuum pump oil vapor on the discharge, the liquid nitrogen cold trap was temporarily removed from the vacuum system. Under these conditions, erratic arcing and carbide formation on the microarc cathode was noted. Reinstallation of the cold trap avoided these difficulties.

Effect of Sample Material on the Microarc

In its application on analysis, the microarc will be coated with sample material, either through evaporation of sample solutions or through a new electrodeposition process to be described in another publication (19). Not unexpectedly, the presence of sample material on the microarc cathode and the existence of sample vapor in the discharge region markedly affects its behavior. In this section, studies will be described which reveal the complex processes which occur as sample material is vaporized from the microarc cathode and moves through the discharge region. In these studies, photometric and temperature measurements were employed, but the most useful information was derived from high speed color motion pictures. Accordingly, let us briefly consider the nature of the information provided by such studies.

Because the 1 ms exposure time of the high speed framing camera was not synchronized with the frequency of the microarc pulsations, all temporal sections of the discharge could be sampled, in a stroboscopic fashion. In each film, several frames were available for each sequential pulsation of the discharge, enabling its behavior to be observed not only on a pulse-to-pulse basis, but also within a single cycle as cathode current rose and fell. Moreover, additional films taken of the same kind of discharge but displaced somewhat in starting time enabled different portions of each cycle to be examined, thereby providing a complete temporal picture of the microarc. In this composite picture, qualitative and semi-quantitative changes in important parameters could be observed and temporally related

through 100 Hz timing marks on each film. The parameters include electrode thermal emission, the extent and color of the glow and arc column and of the excited sample vapor. Three elements (Na, Sr, Al) were chosen to represent a range of chemical and physical behavior in the microarc. A number of physical parameters which govern this behavior are listed in Table 2; the significance of some of these parameters will be discussed in later sections. Conveniently, the three elements chosen are readily distinguished in the high speed color pictures, Na by its characteristic yellow emission, Sr by the well-known red SrOH band, and Al by the green AlO band emission.

Noticeably different behavior was observed during the vaporization of thick and thin films of sample vapor. To form a "thin" deposit of sample material, a small quantity of the chosen element (0.36 nanomoles) was dispensed in the form of a solution onto the microarc cathode. Because this solution droplet evaporated over an area of approximately 0.5 mm^2, this thin coating represented approximately 100 molecular layers of the chosen element. In contrast, "thick" deposits of chosen elements or combinations of elements were formed from 0.8 μg of sample material and corresponded to approximately 1000 molecular layers.

In the following discussion, frame-by-frame events will not be described. Rather, trends in observed volatilization behavior will be outlined and documented when necessary. Although admittedly qualitative, this approach serves best to trace the general character of sample vaporization in the microarc and will form the basis for future quantitative studies. For convenience, volatilization behavior has been broken into two categories, according to the temperature at which each occurs. At low

temperatures, corresponding to the first few cycles of pulsating microarc operation, the wire temperature is everywhere below 1500°C, so that purely thermal sample vaporization and thermionic electron release are relatively insignificant. In contrast, high temperature behavior occurs later in the discharge history and includes phenomena observed when the cathode brightness clearly exceeds that of the anode. Unless otherwise specified, the same conditions were employed in all motion picture studies. Specifically, peak current was 180 mA, electrode gap was 0.5 mm, the discharge atmosphere was 0.8 atm of argon with 1% added hydrogen and the source power was supplied as full wave AC, at 60 Hz.

Low-Temperature Behavior. During the first half-cycle (8 ms) of the discharge, the sample electrode is cathodic; also, the arc column is seen to contain some sample and tends to remain centered in the electrode gap. During this period, the argon glow extends over ~19 mm of the cathode wire as the current peaks and appears much the same as when no sample is present, except for the immediate area where the sample was deposited.

Sodium. Because of its volatility, sodium appears immediately in the first discharge cycle and behaves much the same in either thin or thick deposits. After the first cycle, sodium emission extends around the wire and moves in a sausage shape along the electrode, involving increasing lengths of wire in a reflux-like action until the original deposit area appears exhausted. As late as the 9th discharge cycle, faint sodium emission can be seen near the extremities of the argon glow. However, the maximum intensity appears in the third through fifth cycles, which correlates with an observed maximum drop in the glow voltage. From this

latter observation, it can be concluded that sodium contributes electrons to the discharge. This contribution also produces a rounding of the measured voltage wave forms for the discharge, much as was recorded earlier (cf. Figure 4) for electron contribution through thermionic emission by the cathode.

From the foregoing observaions, the average vaporization rate (Q) of sodium can be estimated assuming that sputtering is the predominant mechanism by which sample is volatilized. All sodium emission had ceased after 100 ms of operation, corresponding to 48 ms of integrated sputtering time. Accordingly, the following expression was used to estimate the vaporization rate of 30 $\mu g\ s^{-1}A^{-1}$:

$$Q = \frac{M_s}{A_s t j}$$

where

M_s is the sample mass,

A_s is the sample area,

t is the integrated time of discharge, 48 ms

j is the average current density of glow over the integrated discharge

Strontium. Like sodium, strontium behaved much the same in either a thin or thick deposit. However, strontium did not appear to move through reflux along the wire as did sodium. Instead, the strontium sample remained localized for the first 6 discharge cycles, with vaporization and excitation in the surrounding glow being quite evident. Further, hot spots of strontium emission were visible and the argon glow did not extend as far

over the cathode wire. After the fourth pulsation (approximately 70 ms) the discharge character changed from a glow to an arc. During this transition, the voltage dropped stepwise to a low level (≈10 V) and the current rose slightly, being limited by a ballast resistance in the power supply.

The discharge behavior can be explained by the exceptionally low work function (cf. Table 2) of strontium oxide. Because thermionic electrons from the heated strontium sample carry an increasingly greater fraction of the discharge current as the sample warms, less current is available to carry the argon glow along the cathode wire. Consequently, the glow beyond the sample area is observed to decrease as the discharge progresses. Arcing, however, is still delayed for several discharge cycles until the sample can warm to a level sufficient for strong thermionic emission. Understandably, localization of the current through arc formation increases the temperature of the strontium deposit even further, leading to a more rapid temperature increase for the sample then measured for the clean cathode wire (cf. Figure 3).

Aluminum. The volatilization of aluminum is of particular interest because of its refractory nature. Even in the efficient Grimm discharge where sputtering in enhanced by operation in an abnormal glow mode, aluminum oxide is reputed to sputter slowly (20). In the present study, thin deposits of aluminum did not begin to yield the characteristic emission of AlO until the 9th discharge cycle (≈150 ms after initiation). However, even at this time the temperature of the microarc cathode was still less than 2000°C, well below the melting point of Al_2O_3 (23). Allowing the

same sample to cool and re-initiating the discharge again produced no visible AlO emission until after 10 cycles of the discharge had occurred, indicating the importance of cathode heating to aluminum volatilization.

In contrast, thick deposits of aluminum yielded visible emission of AlO on the first cycle of the discharge. Even during this first cycle, the arc column anchored to the extreme edges of the dried deposit area, which remained relatively dark, while the glow extended over the remaining cathode area. Clearly, the dielectric properties of the oxide coating plays an important role in determining the character of the discharge on the cold electrode. This anchored arc column was observed to be spatially unstable and moved from one side of the deposit to the other during each discharge cycle. Despite the intense appearance of the arc column, the voltage-time behavior of the system is still characteristic of a glow.

An attempt was made to ascertain whether a refractory element such as aluminum would migrate through sputtering during the early stages of the discharge. In these experiments, extreme care was taken to deposit the aluminum sample on the inside bend of the cathode wire, while the anode was placed nearest the outside of the bend. Short bursts of four discharge cycles then were allowed to occur. After each burst the cathode was allowed to cool, and the cycle repeated. Observations of the resulting emission were made both visually using a cathetometer focused on the microarc cathode and with a photodiode array upon which the discharge was imaged. In these measurements, an arc column was observed to immediately form and anchor to a small area (ca. 50 μm dia.) on the cathode; this area immediately became red-hot (ca. 1000°C) while the glow extended over the entire bare wire.

However, aluminum emission was not observed until the third repetition of these four-cycle bursts, indicating a significant amount of time is necessary for aluminum to migrate around the wave to the vicinity of the arc column, where rapid vaporization can occur. This suggests that sputtering of the cold aluminum sample is inefficient, as if the sample deposit itself cannot support the glow discharge.

Following the initial appearance of aluminum emission, similar emission could be seen when the hot counter electrodes became cathodic, indicating that the metal is cycled between the two electrodes. This observation reinforces motion picture data which reveal recondensation of all test elements on the heated anode, followed by quite uniform vaporization on the second half-cycle.

Multielement Deposits. When the three test elements were added in a thin deposit to the electrode, no interelement effects were observed. Instead, motion pictures of the first 10 cycles of the discharge revealed that each element behaved much as it did when alone. As expected, sodium and strontium were observed to volatilize more rapidly than aluminum and tended to migrate to distant parts of the cathode. By the third cycle, the discharge voltage had dropped somewhat and the sausage-like cloud of glowing vapor had developed fully; by the seventh cycle the individual characteristic color of each element was easily distinguishable. This behavior suggests that the more volatile sodium and strontium had fractionally distilled and the remaining sample deposit consisted primarily of aluminum. On the ninth discharge cycle, the glow relaxed to an arc-like

discharge and the tenth cycle began as an arc. If this same, now depleted, sample were then allowed to cool and the discharge re-initiated, the glow-to-arc transition occurred earlier (on the eight cycle), suggesting that the volatilization of sodium and strontium from the cathode slowed its original rate of heating somewhat. Such ablative cooling is one of the stronger interelement effects which occur in the microarc discharge.

The High Temperature Behavior. When the cathode wire temperature reaches 1400°C, sodium is no longer present and strontium simply continues to arc in the manner previously described. (The case of a reduced-current discharge, in which strontium does not arc, is discussed in the next section.) Therefore, only the behavior of aluminum is discussed here.

In contrast to localized spatially unstable discharge formed on the cold, aluminum-coated electrode, the hot electrode exhibits an increasingly uniform emission pattern which is distributed over ever larger areas of the wire. In addition, the arc column centralizes in the gap and appears more diffuse. This uniform, more diffuse emission is attributable to the even redistribution of aluminum in a layer thin enough as to sustain a glow, in contrast to its earlier, insulating character.

Interestingly, aluminum vaporization from the hot cathode appeared to be caused by a cooperative process involving both the wire temperature and sputtering. The process, which could be observed during single discharge pulsations, was most obvious in the last stages of vaporization, when the only aluminum remaining was recondensed material located far along the cathode wire, near extremities of the glow. As the pulse of current approached its maximum value (on a millisecond time scale) the glow crept

along the incandescent wire and eventually reached the cooler region where aluminum was still present. When the glow had extended a short distance (ca. 2 mm) into this region, aluminum vapor appeared (as evidenced by its emission) but only from a narrow (ca 1 mm) region where the wire was hottest (as evidenced by relative brightness). Concurrent with the appearance of aluminum emission, the glow immediately contracted, suggesting the involvement of the glow in the volatilization event. The localized behavior of this vaporization further suggests that some minimum cathode temperature must be achieved before the rate of sputtering is greatly enhanced.

Similar temperature dependent sputtering enchancements with tantalum and tungsten (21) have been attributed to chemical effects. Unfortunately, we have not been able to accurately determine the temperature, and further studies will be necessary to ascertain if, for example, the onset of tungsten oxide vaporization (cf. Fig. 7) participates in causing a chemical enhancement of aluminum vaporization.

For practical purposes, we may conclude that since discontinuous changes in the vaporization are to be expected as the wire temperature rises, integration of the analytical signal must be employed.

Effects with Uniform Deposits

The preceeding observations of uniform emission from recondensed material suggested placing the sample on the wire support in the form of a thin, uniform deposit in hope of preventing the unstable arc-like behavior observed with localized, dried deposits.

To test this idea, a high voltage electrodeposition technique (19) was used to deposit a equimolar mixture of strontium and aluminum as the oxides. The thickness of deposits over a 4 mm length of wire loop varied from 10-20 molecular layers (~.4 nmol) to 100-200 molecular layers (~4 nmol). To further prevent arc formation from strontium, the current was limited to 78 mA in the studies described here.

The discharge was observed to occur in five stages, which are discussed in the sections that follow. Because the bare wire surface is not available to support the discharge, it is not surprising that the general behavior, particularly the first two stages, differs greatly from the preceeding descriptions.

The First Stage. The discharge began the appearance of a columnar arc across the smallest interelectrode distance. With the thicker samples, a spot located inside the cathode loop, where the sample deposit is thin, often was the initial point of discharge. The voltage waveform during the first few cycles of the discharge, shown in Fig. 8, is characterized by a high breakdown voltage and rapid, oscillation reminiscent of the charging and discharging of a capacitor. This behavior, and the limiting voltages (30-60 V) observed are similar to the little-studied spray-glow discharge described by a few workers (22,23) and in reviews (5,24). Field emission is an important feature in this type of glow. In practice, the RF noise evident here may affect the instrumentation. Also, the high voltage requirement for breakdown limits the practical sample thickness. The initiation for thicker samples was often sporadic. These problems need not be serious, since they may obviously be overcome by resistively heating the

sample electrode. For example, Fig. 8 shows that the heating from the discharge alone was sufficient to cause the normal glow characteristic of the second stage to be achieved within 8 to 10 cycles.

The Second Stage. The initial diameter of the discharge spot was measured to be 0.2 mm, so that it could be inferred that the glow current density was in the order of 200 A/cm^2. Although it would seem that the sample would be quickly vaporized by such a concentrated discharge, the spot was observed to wander only occasionally over a period of 60-100 cycles on the thicker samples. The remaining sample surface remained relatively cold. Therefore it was apparent that the discharge was ineffective in heating the wire. Ablative cooling by the vaporizing sample helps to explain the absorption of the energy from the discharge. This explanation is consistent with the behavior with thin samples, which showed little tendency to maintain the spot discharge. Instead, the spot immediately expanded into the cylindrical glow of the third stage.

The Third Stage. The transition from a spot to a cylindrical glow took place within a few cycles, and the glow continued to increase uniformly in length from 0.5 to 3 mm within 200 ms. The corresponding area of the wire increased in temperature to 1200-1400^{o}C.

This behavior supports the expectation that hot uniform depositions will support a glow free of the arc column instabilities that have been previously described.

The Fourth Stage. This stage was characterized by the appearance of hot spots that were 0.3 to 0.5 mm in diameter. From the previous descriptions, it is clear that strontium was responsible, and that arc

formation was restrained by the current limits imposed in this study. The hot spots were observed to wander sporadically at first, but toward the end of this stage, the wandering occurred with increasing rapidity and surface coverage. This was suggestive of the vaporization of the last molecular layers.

The hot spots and wandering can be attributed, as before, to the greater availability of electrons from SrO as opposed to the tungsten wire surface. Because the vaporization requires less time as the sample is depleted, the spots wander to fresh sources of sample more quickly. Recondensation must play an important role in this mechanism, because the hot spots return to the same surface locations several times. It is predictable that if the work functions of the sample and tungsten are more similar, the last molecular layers will be removed less efficiently, and slowly drifting analytical signals will be observed. Preliminary studies with CaO confirm that such drift is indeed observed. To overcome this sluggish vaporization, the temperature of the wire must be made to rise. This occurs in the fifth and last stage.

The Fifth Stage. The removal of the last traces of sample is marked by the disappearance of hot spots, and by a more uniform extended glow over a much hotter wire. This behavior is identical to that observed with localized dried deposits. A removal of the last vestiges of recondensed sample is observed. Clearly, thermal processes are most important in this last stage.

From the foregoing descriptions, we can conclude that the duration and atomization efficiency during each stage of the discharge is either determined or regulated by the sample placement and composition.

SUMMARY AND CONCLUSIONS

It is interesting and practically significant to compare the behavior of the microarc to that of a wire or ribbon electrothermal atomizer. With the latter kind of device, rapid resistive heating of the substrate is employed to achieve high rates of sample volatilization. The resulting atom density and analytical sensitivity tend to improve as the thermal ramp more nearly resembles a step-function. However, because of thermal lag across a sample deposit, vaporization can occur first at the wire-sample interface, which in turn will disrupt the outer, cooler portions of the sample. Such behavior leads to inefficient atomization and occasional loss of sample material. In contrast, the microarc discharge causes vaporization to occur from the sample surface *inward* by a bombardment process. Furthermore, it provides an excellent environment to atomize vaporizing molecular species. As the improved sensitivity and detection limits (3) seem to indicate, atomization promises to be inherently more efficient in a discharge-dominated microarc.

Unfortunately, as this study shows, the manner in which the discharge couples to the sample can be a source of spatial and atomization non-uniformity that is not important in purely thermal atomizers. Furthermore, because of non-uniform heating of the wire support,

recondensation of the sample onto the wire must be considered. Of course, this latter problem is minimized by the use of a gas flow over the discharge, such as would be required to transport the sample atoms to a secondary source of excitation (e.g. such as the microwave induced plasma).

The effects of spatial and atomization instability can be reduced by the usual practice of integrating the sample signal over the whole course of the discharge. However, even then arc formation can produce errors with its attendant intense background emission, excessively high sample emission and the possible explosive fragmentations of sample deposits. Fortunately, arc formation, which is sample dependent, can be controlled in several ways. The use of hydrogen as an additive aids in providing better thermal diffusion, as well as providing reducing conditions. Recent work (25) indicates that the use of helium with the microarc produces smoother discharges. Helium is well-known to be effective for thermal conduction. Another way is to lower the heating rate by reducing the discharge current, decreasing the duty factor, or employing a cooling gas sheath. Also, as this study describes, the use of uniform sample deposits has the merit of localizing the discharge and maximizing the effect of ablative cooling by the sample to prevent the wire temperature from rising too quickly. Although these later techniques would result in lowered vaporization rates for the sample as a whole they allow larger samples to be used, thereby increasing the dynamic range for determinations.

The potential difficulties with discharge initiation using uniform deposits require further study. The present study noted that initiation took place at thin spots which may have been fortuitous. In addition, RF noise associated with the poorly understood spray-glow discharge may cause instrumental difficulties.

Some aspects of the discharge behavior, such as the wandering of hot spots, appear related to the relative electron availability from the sample compounds. This behavior suggests the use of additives with low work functions, such as SrO, to better direct the discharge to the sample and thereby improve the vaporization of refractory elements. This suggestion is easily implemented with the electrodeposition technique used in this study which is most quantitative when carriers are employed.

ACKNOWLEDGMENTS

The authors are grateful for the assistance of John Elliot in the design and construction of the power supply.

CREDITS

One of the authors (G.M.H.) gratefully acknowledges support of part of this work by the National Science Foundation and the Office of Naval Research.

LITERATURE CITED

1. V. A. Fassel and R. N. Kniseley, Anal. Chem. 46, 1110A (1974)
2. G. S. Hurst, M. H. Nayfeh, and J. P. Young, Phys. Rev. A 15, 2283 (1977).
3. L. R. Layman and G. M. Hieftje, Anal. Chem. 47, 194 (1975).
4. G. Francis, in Handbuch der Physik, Vol. 22, Springer, Berlin, 1956. pp. 53-208.
5. A. v. Engel, Ionized Gases, Clarendon Press, Oxford, 1955.
6. F. Llewelyn-Jones, The Glow Discharge, Methuen, London; Wiley, New York, 1966.
7. J. R. Acton and J. D. Swift, Cold Cathode Discharge Tubes, Academic Press, New York, 1963.
8. P. J. Slevin and W. W. Harrison, Appl. Spectroscopy Reviews 10, 201 (1975).
9. W. S. Boyle and F. E. Haworth, Phys. Rev. 101, 935 (1956).
10. W. A. Gambling and H. Edels, Brit. J. Appl. Phys. 5, 36 (1954).
11. A. V. Engel, R. Seeliger, and M. Steinbeck, Z. Physik 85, 144 (1933)
12. E. Badareu, I. Popescu, and I. Iova, Ann. der Physik 5, 308 (1960).
13. I. Reif, V. A. Fassel, and R. N. Kniseley, Spectrochim. Acta 28B, 105 (1973).

14. B. D. Adcock and W. E. G. Plumbtree, J. Quant. Spectrosc. Radiat. Transfer 4, 29 (1964).
15. A. N. Shteinberg, Zh. Priklad. Spect. 2, 385 (1965).
16. W. Weltner, Jr. and D. McLead, Jr., J. Molec. Spectroscopy 17, 276 (1965).
17. F. E. Haworth, J. Appl. Phys. 22, 606 (1951).
18. O. Krikorian, Lawrence Livermore Laboratory, Livermore, CA, Private communication.
19. R. I. Bystroff and M. Weiner, Anal. Chem., submitted - 1978.
20. D. S. Gough, P. Hannaford, and A. Walsh, Spectrochim. Acta 28B, 197 (1973).
21. U. A. Arifov, V. A. Shustror and A. K. Ayukhanov, Proc. Tenth Int. Conf. Phen. Ion. Gases, Oxford, England (1971) p. 67. D. Parsons, Oxford, England.
22. F. E. Haworth, Phys. Rev. 80, 223 (1950).
23. A. Guntherschultz and H. Frick, Z. Physik 86, 821 (1933).
24. P. F. Little, Handbuch der Physik, Vol. 21, Springer, Berlin, 1956. p. 634.
25. A. T. Zander and G. M. Hieftje Anal. Chem., in press-1978.

FIGURE CAPTIONS

Fig. 1. Block diagram of the microarc apparatus and photometric monitoring system.

Fig. 2. Cross-section of the electrode assemblies. (a) Counter electrode (cathode) assembly, showing the 2 mL sawed-off syringe, 1, with Ni-alloy feedthroughs, 2, and hairpin electrode, 3. The threaded brass coupling, 4, compresses a brass ring, 5, onto a neoprene O-ring, 6. (b) Sample electrode assembly, showing the sealed electrode, 3, a Swagelok fitting, 4, which compress a small O-ring, 6.

Fig. 3. Tungsten cathode temperature in an 0.8 atm argon glow discharge for half-wave rectified power, I_{max} = 180 mA.

Fig. 4. Voltage-time waveforms in a 60 Hz argon glow discharge:

a) normal glow showing a typical cold breakdown,

b) hot electrode showing a much reduced breakdown,

c) arc character evident at low currents,

d) arc transition occurring in the second half of a cycle,

e) arc prevails over most of the cycle, the early portion is in the transition region.

Fig. 5. Argon (415.8 nm) and tungsten (400.9 nm) atomic emission in the negative glow as a function of discharge power.

Fig. 6. Argon (415.8 nm) and tungsten (400.9 nm) atomic emission as a function of anode temperature. The discharge power is held constant, while the anode loop power is varied by 40%.

Fig. 7. Argon and tungsten atomic emission in the negative glow as a function of time of discharge. A. Argon (415.8 nm). B. Tungsten (400.9 nm) with oxygen present. C. Tungsten emission with 1% H_2 added. The noise and pulsations have been removed to show the general trends and magnitudes.

Fig. 8. Voltage characteristics during the initial discharge over uniform deposits.

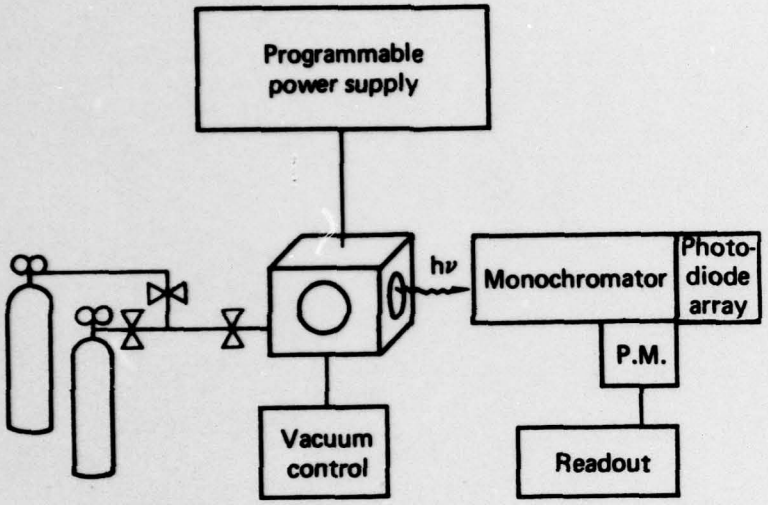

Figure 1

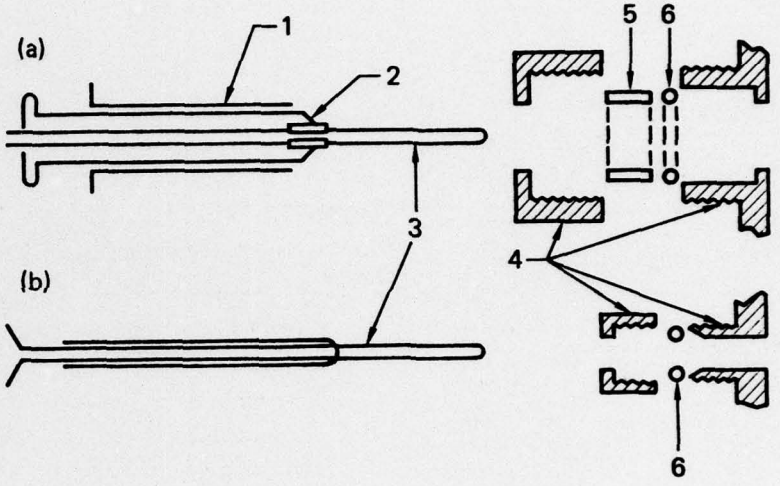

Figure 2

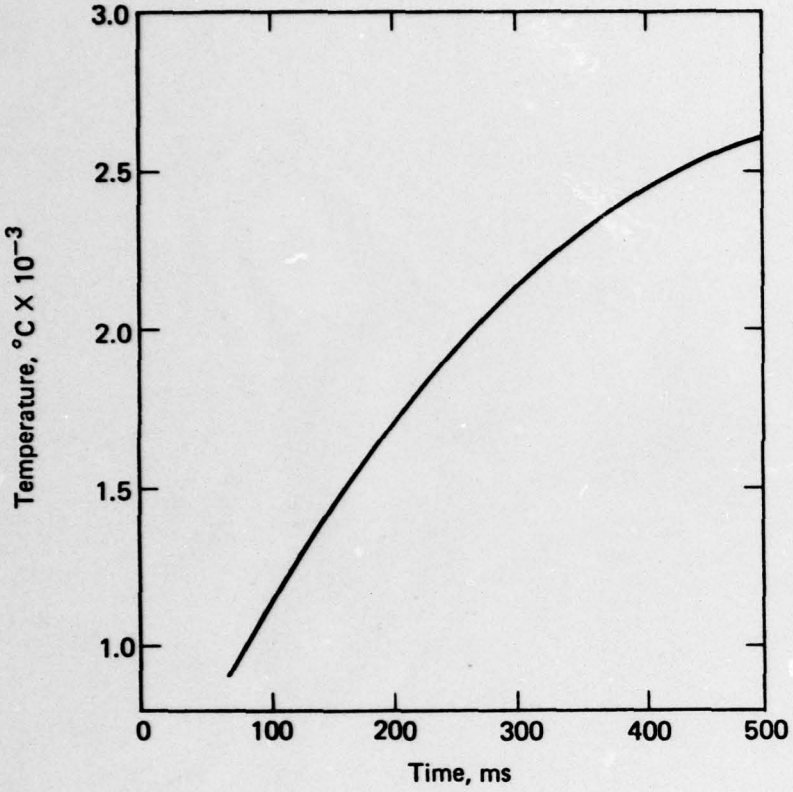

Figure 3

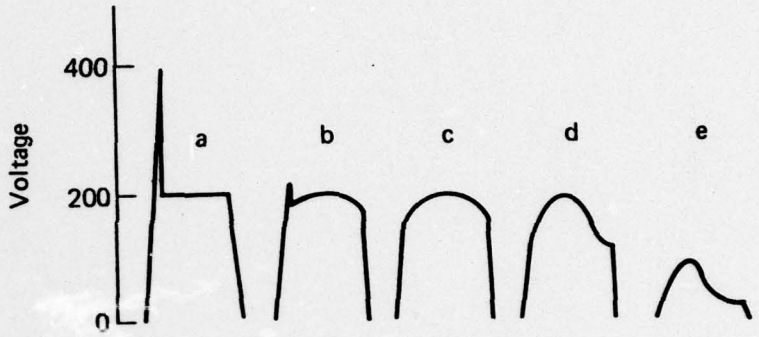

Figure 4

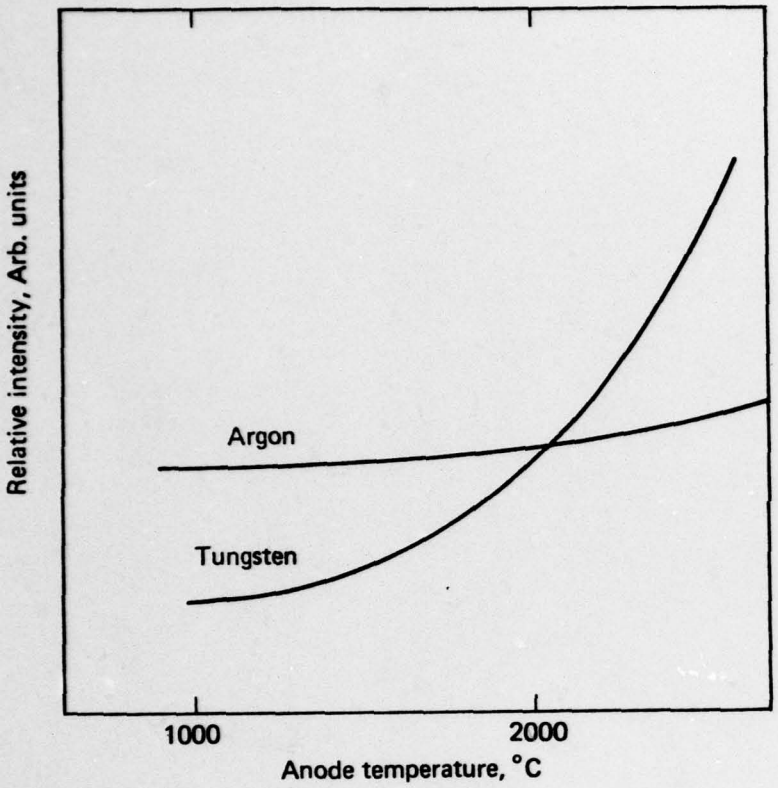

Figure 5

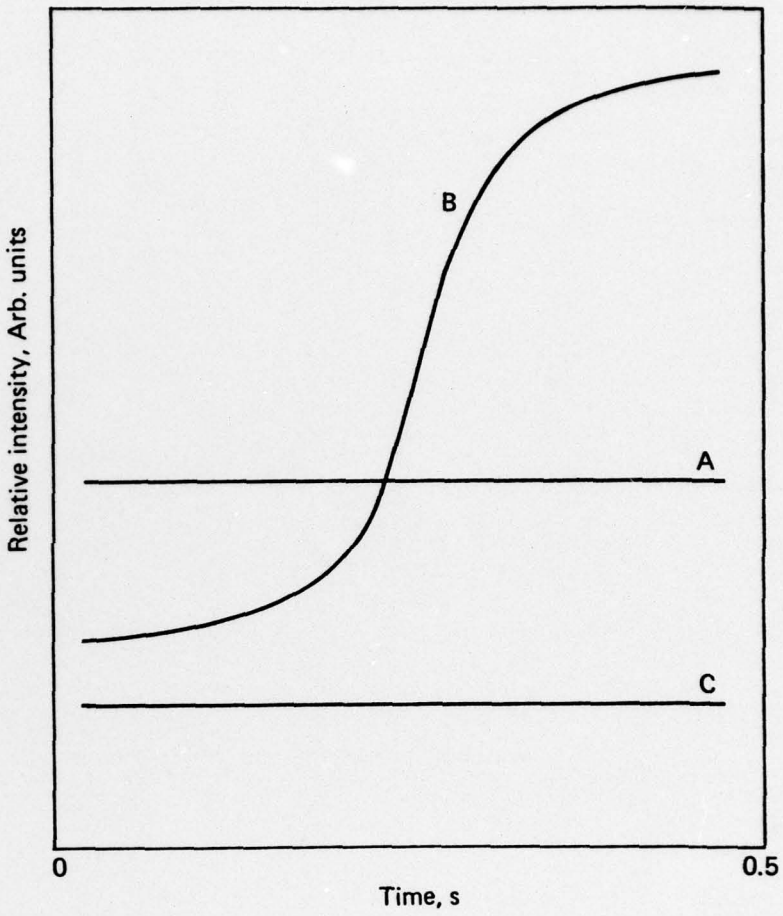

Figure 6

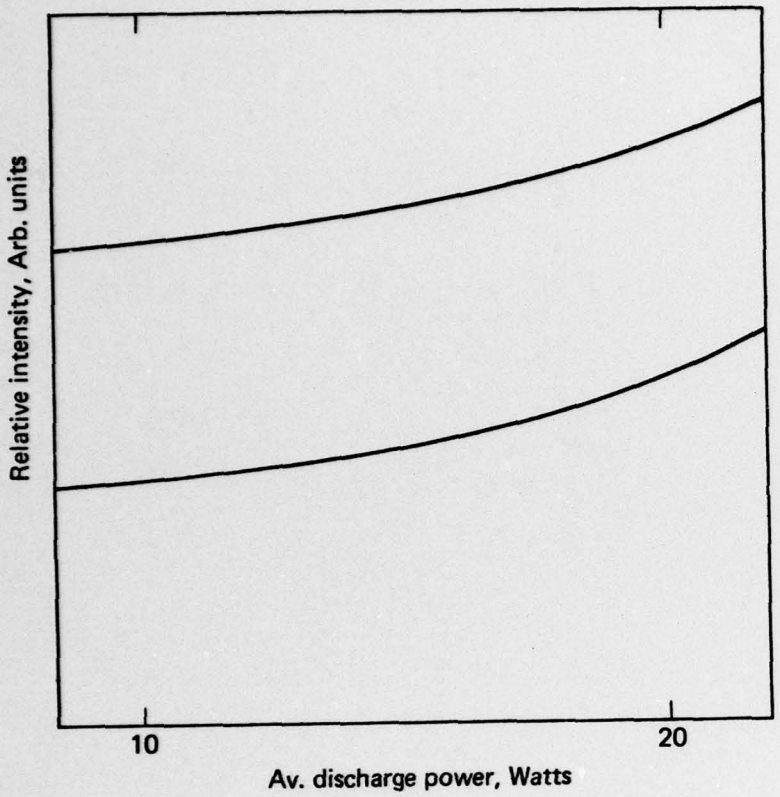

Figure 7

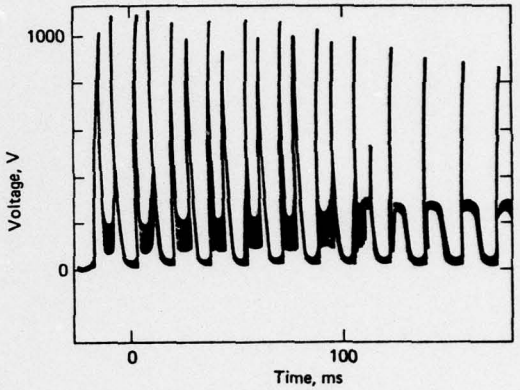

Figure 8

Table 1. Operating Conditions and Characteristics of the Tungsten Wire Microarc in Argon.

Electrode diameter	0.25 mm
Electrode gap	0.2-2.0 mm
Pressure	0.8-1.0 atm. (8-10 kPa)
Glow voltage*	180-220 V
Glow current	40-200 mA
Current density	1.2 A cm^{-2}
Glow distance	10 μm
Mean free path	100 nm
E/P	240 V cm^{-1} $torr^{-1}$
Cathode Temperature	<3000°C
Glow Excitation Temperature	5000±200°K

*Equivalent to the cathode fall for small gaps.

Table 2. Physical parameters for the species of interest.

Species	M.P., °C	B.P., °C	Work function $\times 10^{19}$ J	Resistivity ohm•m	@T, °K
NaCl	801	1413			
NaOH	318	1390			
Al_2O_3	2045	2980	7.75	10^{14}	287
				290	2083
SrO	2430	3000	2.24	40	1473
CaO	2580	2850	4.32	20	1643
Al	660	2467	4.2		
Sr	769	1384			
WO_2	1500	1430	7.94		
W	3410	5660	4.54		

TECHNICAL REPORT DISTRIBUTION LIST

	No. Copies
Office of Naval Research Arlington, Virginia 22217 Attn: Code 472	2
ONR Branch Office 536 S. Clark Street Chicago, Illinois 60605 Attn: Dr. Jerry Smith	1
ONR Branch Office 715 Broadway New York, New York 10003 Attn: Scientific Dept.	1
ONR Branch Office 1030 East Green Street Pasadena, California 91106 Attn: Dr. R. J. Marcus	1
ONR Branch Office 760 Market Street, Rm. 447 San Francisco, California 94102 Attn: Dr. P. A. Miller	1
ONR Branch Office 495 Summer Street Boston, Massachusetts 02210 Attn: Dr. L. H. Peebles	1
Director, Naval Research Laboratory Washington, D.C. 20390 Attn: Code 6100	1
The Asst. Secretary of the Navy (R&D) Department of the Navy Room 4E736, Pentagon Washington, D.C. 20350	1
Commander, Naval Air Systems Command Department of the Navy Washington, D.C. 20360 Attn: Code 310C (H. Rosenwasser)	1

	No. Copies
Defense Documentation Center Building 5, Cameron Station Alexandria, Virginia 22314	12
U.S. Army Research Office P.O. Box 12211 Research Triangle Park, N.C. 27709 Attn: CRD-AA-IP	1
Naval Ocean Systems Center San Diego, California 92152 Attn: Mr. Joe McCartney	1
Naval Weapons Center China Lake, California 93555 Attn: Head, Chemistry Division	1
Naval Civil Engineering Laboratory Port Hueneme, California 93041 Attn: Mr. W. S. Haynes	1
Professor O. Heinz Department of Physics & Chemistry Naval Postgraduate School Monterey, California 93940	1
Dr. A. L. Slafkosky Scientific Advisor Commandant of the Marine Corps (Code RD-1) Washington, D.C. 20380	1
Office of Naval Research Arlington, Virginia 22217 Attn: Dr. Richard S. Miller	1

TECHNICAL REPORT DISTRIBUTION LIST

	No. Copies
Dr. M. B. Denton University of Arizona Department of Chemistry Tucson, Arizona 85721	1
Dr. G. S. Wilson University of Arizona Department of Chemistry Tucson, Arizona 85721	1
Dr. R. A. Osteryoung Colorado State University Department of Chemistry Fort Collins, Colorado 80521	1
Dr. B. R. Kowalski University of Washington Department of Chemistry Seattle, Washington 98105	1
Dr. I. B. Goldberg North American Rockwell Science Center P.O. Box 1085 1049 Camino Dos Rios Thousand Oaks, California 91360	1
Dr. S. P. Perone Purdue University Department of Chemistry Lafayette, Indiana 47907	1
Dr. E. E. Wells Naval Research Laboratory Code 6160 Washington, D.C. 20375	1
Dr. D. L. Venezky Naval Research Laboratory Code 6130 Washington, D.C. 20375	1
Dr. H. Freiser University of Arizona Department of Chemistry Tuscon, Arizona 85721	
Dr. Fred Saalfeld Naval Research Laboratory Code 6110 Washington, D.C. 20375	1
Dr. H. Chernoff Massachusetts Institute of Technology Department of Mathematics Cambridge, Massachusetts 02139	1
Dr. K. Wilson University of California, San Diego Department of Chemistry La Jolla, California 92037	1
Dr. A. Zirino Naval Undersea Center San Diego, California 92132	1
Dr. John Duffin United States Naval Post Graduate School Monterey, California 93940	1
~~Dr. G. M. Hieftje~~ ~~Department of Chemistry~~ ~~Indiana University~~ ~~Bloomington, Indiana 47401~~	1
Dr. Victor L. Rehn Naval Weapons Center Code 3813 China Lake, California 93555	1
Dr. Christie G. Enke Michigan State University Department of Chemistry East Lansing, Michigan 48824	1